Journal of Quality Measurement and Analysis
e-ISSN: 2600-8602
https://doi.org/10.17576/jqma.2202.2026.05

JQMA 22(2) 2026, 67-89
http://www.ukm.my/jqma

BIFURCATION ANALYSIS AND BISTABILITY IN A PREDATOR-PREY MODEL WITH COSNER-TYPE FUNCTIONAL RESPONSE AND MICHAELIS-MENTEN PREY HARVESTING

(*Analisis Bifurkasi dan Dwikestabilan dalam Model Mangsa-Pemangsa dengan Fungsi Tindak Balas Jenis Cosner dan Penuaian Mangsa Jenis Michaelis-Menten*)

HUI YI CHEN & TAU KEONG ANG*

ABSTRACT

Long-term population survival in a predator-prey model often depends on how a species responds to predation and harvesting within its ecosystem. To capture these dynamics, this research investigates a two-dimensional predator-prey model incorporating a Cosner-type functional response and Michaelis-Menten-type nonlinear prey harvesting. The model reflects cooperative hunting behaviour among predators and the saturation effect in prey harvesting, which can significantly influence population dynamics. The model possesses three types of equilibria, namely extinction, predator-free and coexistence equilibria. Bistability is observed at a high harvesting saturation rate, indicating that initial conditions play a crucial role in determining the long-term outcomes for both species. The local stability of each equilibrium point is analysed using the Jacobian matrix and Routh-Hurwitz criterion. Bifurcation analysis is performed on the system using Sotomayor's theorem and the Hopf bifurcation theorem. Numerical bifurcation analysis is carried out by plotting bifurcation diagrams and time series using MATLAB and MatCont software packages. It is found that, as the harvesting saturation rate increases, the model undergoes several codimension-one bifurcations, including saddle-node, pitchfork and Hopf bifurcations. The results show that a high harvesting saturation rate enhances the likelihood of coexistence, whereas a low harvesting saturation rate eventually leads to the extinction of both populations. These results highlight the importance of controlling the harvesting saturation rate to ensure long-term coexistence and prevent population extinction.

Keywords: bistability; predator-prey model; Cosner-type functional response; Michaelis-Menten prey harvesting; bifurcation

ABSTRAK

Kemandirian jangka panjang populasi dalam model mangsa-pemangsa sering bergantung kepada cara sesuatu spesies bertindak balas terhadap pemangsaan dan penuaian dalam ekosistemnya. Bagi menggambarkan dinamik ini, kajian ini menyiasat model mangsa-pemangsa dua dimensi yang menggabungkan fungsi tindak balas jenis Cosner dan penuaian mangsa tak linear jenis Michaelis-Menten. Model ini mencerminkan tingkah laku memburu secara koperatif dalam kalangan pemangsa dan kesan ketepuan dalam penuaian mangsa, yang boleh mempengaruhi dinamik populasi secara signifikan. Model ini mempunyai tiga jenis titik keseimbangan, iaitu keseimbangan kepupusan, tanpa pemangsa dan kewujudan bersama. Fenomena dwikestabilan diperhatikan pada kadar ketepuan penuaian yang tinggi, menunjukkan bahawa keadaan awal memainkan peranan penting dalam menentukan hasil jangka panjang bagi kedua-dua spesies. Kestabilan setempat bagi setiap titik keseimbangan dianalisis menggunakan matriks Jakobian dan kriteria Routh-Hurwitz. Analisis bifurkasi dijalankan terhadap sistem menggunakan teorem Sotomayor dan teorem bifurkasi Hopf. Analisis bifurkasi secara berangka dijalankan dengan memplot rajah bifurkasi dan siri masa menggunakan perisian MATLAB dan MatCont. Hasil kajian menunjukkan bahawa apabila kadar ketepuan penuaian meningkat, model ini mengalami beberapa bifurkasi kodimensi satu, termasuk bifurkasi saddle-node, pitchfork dan Hopf. Hasil kajian juga menunjukkan bahawa kadar ketepuan penuaian yang tinggi meningkatkan kebarangkalian kewujudan bersama, manakala kadar ketepuan penuaian yang rendah akhirnya

membawa kepada kepupusan kedua-dua populasi. Dapatan ini menekankan kepentingan pengawalan kadar ketepuan penuaian bagi memastikan kewujudan bersama jangka panjang dan mencegah kepupusan populasi.

Kata kunci: dwikestabilan; model mangsa-pemangsa; fungsi tindak balas jenis Cosner; penuaian mangsa jenis Michaelis-Menten; bifurkasi

1. Introduction

Predator-prey interactions are important for maintaining ecosystem balance, but these interactions are often affected by habitat destruction and overharvesting. Such human activities can disrupt predator-prey dynamics by disturbing the balance between species, affecting ecological systems and accelerating population extinction. When species are unable to withstand predation and external factors such as harvesting, their long-term survival is threatened. Hence, predator-prey models are useful tools for studying these effects and predicting possible population outcomes. Recent developments in nonlinear mathematical modelling have also shown that analytical and numerical techniques remain important for understanding the behaviour of complex dynamical systems (Eshkuvatov *et al.* 2025, 2021).

One of the crucial elements in predator-prey models is the functional response. The concept of functional response was proposed by Holling (1959), which is a function that represents the rate at which prey is consumed by predators. Functional responses have been widely used and extended to incorporate ecological complexities. These extensions highlight how various forms of functional response can significantly affect system dynamics.

Classical Holling-type I to IV functional responses offer a foundational framework for modelling consumption rates. However, these functional responses depend solely on prey density (Debnath *et al.* 2022), limiting their applicability in more complex predator-prey interactions. One of the complexities arises from cooperative hunting, where predators form groups to increase hunting efficiency and success rates. This behaviour is observed in species such as wolves, which hunt in packs when targeting strong or harmful prey (Mech 1970). Such cooperation implies that predator density can also influence consumption rates. To address this, Cosner *et al.* (1999) proposed a hunting cooperation functional response, $F(n, p)$, that depends on both prey density n and predator density p. The Cosner-type functional response takes the following form:

$$F(n, p) = \frac{Se_0np}{1 + hSe_0np}. \tag{1}$$

The coefficient S reflects the quantity of prey taken by a predator per encounter, e_0 is the time necessary to handle each prey, and h is the overall encounter coefficient between predator and prey. Equation (1) is also known as an increasing functional response, because hunting efficiency increases monotonically with both predator and prey populations. This functional response has been shown to exhibit interesting dynamical behaviours. Such behaviours include multistability and various high-dimensional bifurcations when incorporated into models with logistic growth (Ryu *et al.* 2018), Leslie-type prey growth (Shang *et al.* 2021a), and the model considering the Allee effect (Kumbhakar *et al.* 2023).

One further improvement of the model is the incorporation of harvesting activities. Harvesting can serve as a control strategy, especially when population imbalances become extreme and threaten the survival of interacting species. Hence, some studies incorporate constant harvesting (Shang *et al.* 2021b) and proportional harvesting (Mulugeta *et al.* 2024) alongside the Cosner-type functional response. Their results reveal that harvesting can significantly affect population survival and lead to interesting bifurcation structures. Although these approaches

offer valuable insights, constant harvesting, H, may lead to overexploitation when prey density is low, whereas proportional harvesting, $H(n) = qEn$, assumes unlimited harvesting effort, where q denotes the catchability coefficient and E denotes the harvesting effort.

To address these limitations, Michaelis-Menten-type nonlinear harvesting, proposed by Clark and Mangel (1979), serves as a more biologically realistic alternative, as it accounts for saturation effects and finite harvesting capacity (Kashyap *et al.* 2023; Xie *et al.* 2021). Michaelis-Menten-type nonlinear harvesting takes the form

$$H(n) = \frac{qEn}{m_1 E + m_2 n}, \tag{2}$$

where q is the catchability coefficient, E is the intensity of harvesting, n represents the harvested species, and m_1 and m_2 represent saturation effects where harvesting efficiency levels off due to limitations in equipment, manpower or ecological resistance (Moussaoui & Auger 2021). As $n \to \infty$, the harvesting function satisfies

$$H(n) \to \frac{qE}{m_2},$$

while for large effort levels, $E \to \infty$,

$$H(n) \to \frac{qn}{m_1}.$$

These limiting behaviours indicate that the harvesting process exhibits saturation with respect to both stock size and harvesting effort. At high effort levels, the parameter m_1 scales with the ratio between stock size and the corresponding harvesting rate, whereas at high stock levels, m_2 scales with the ratio between effort and the harvesting rate. Consequently, Michaelis-Menten-type harvesting overcomes the shortcomings of constant and linear harvesting by introducing saturation effects that ensure bounded harvesting rates and effort levels.

Despite growing interest in each of these mechanisms, the combined effects of Cosner-type functional responses and nonlinear Michaelis-Menten-type harvesting have yet to be thoroughly investigated. This gap motivates the present paper, which analyses the dynamics of predator-prey interactions under the influence of both mechanisms. The objective is to examine how their combination affects the stability and bifurcation structure of the system. The paper is structured as follows. Section 2 provides a review of the relevant literature. Section 3 introduces the model, followed by an analysis of the equilibrium points and their stability in Section 4. In Section 5, bifurcation analysis of the system is carried out. Section 6 presents the numerical simulation. Section 7 discusses the main results and their ecological implications. Finally, Section 8 concludes the study.

2. Literature Review

Numerous predator-prey models have been developed based on Holling-type functional responses, laying the foundation for theoretical studies on predator-prey dynamics. One notable advancement in predator-prey modelling is the transition from prey-dependent to predator-dependent functional responses, such as the Beddington-DeAngelis-type functional response (Shao & Kong 2022) and the Crowley-Martin-type functional response (Roy & Tiwari 2025). However, these functional responses mainly focus on intraspecific competition among predators due to predator crowding. In contrast, Berec (2010) was among the first to reinterpret predator-dependent functional responses as mechanisms that reflect foraging facilitation among predators. This offers a new perspective that better captures group hunting behaviours observed in nature.

Extending this idea, Alves and Hilker (2017) introduced a linear functional response to capture predator cooperation. However, this functional response assumes that cooperation increases indefinitely as predator density increases, which is biologically unrealistic. For instance, MacNulty *et al.* (2014) observed that wolf hunting success increased with group size when targeting difficult prey but levelled off for easier prey. This suggests that cooperative effects among predators may saturate. Therefore, a linear increase in cooperation is an unrealistic assumption. The Cosner-type functional response proposed by Cosner *et al.* (1999) improves this limitation by incorporating a saturation effect that limits cooperation at high predator densities. The Cosner-type functional response is derived based on the spatial grouping of predators, where a group of predators moves in straight foraging lines while searching for prey. When one predator encounters a group of prey, it transmits a signal to other predators, triggering group hunting. While this signalling improves hunting efficiency at first, too many predators can slow down signal transmission and reduce hunting efficiency. This makes the Cosner-type functional response a more realistic approach for modelling cooperative hunting. Further studies, such as Yang *et al.* (2022) and Kumbhakar *et al.* (2023), have used this approach in ecological modelling.

While cooperative hunting improves our understanding of predator-prey interactions, harvesting is an external factor that can significantly shape population dynamics. The inclusion of harvesting can change the overall dynamics of a model, leading to the survival or extinction of species. For instance, Ryu *et al.* (2018) proposed a predator-prey model without considering any harvesting activities. Their analysis proved the presence of an extinction equilibrium point, which can be stable within a certain range of parameter values. This suggests that both populations may become extinct when conditions are unfavourable. One notable study by Shang *et al.* (2021b) extended the same model by introducing constant prey harvesting, and the results show that the extinction equilibrium no longer exists. Since extinction is not possible in that model, this implies that the prey population persists regardless of parameter values. However, such behaviour may not fully capture biological reality, since a high harvesting rate can threaten population survival (Majumdar *et al.* 2021).

To address this limitation, many studies have adopted Michaelis-Menten-type harvesting to reflect real-world constraints. In contrast to constant harvesting, Michaelis-Menten-type harvesting incorporates saturation effects, where harvesting efficiency levels off due to effort saturation, gear capacity or ecological factors (Moussaoui & Auger 2021). Evidence from fisheries indicates that catch rates may saturate at high levels of harvesting because of limited storage space and the need for intermittent fishing operations. Hence, incorporating saturation effects provides a more realistic representation of harvesting and can lead to more complex and varied population dynamics than constant and linear harvesting. Mortuja *et al.* (2025) considered Michaelis-Menten-type harvesting in a predator-prey model. The results indicated that increasing the harvesting rate can lead to population extinction and complex dynamics such as Hopf bifurcation and multistability. This highlights the role of nonlinear harvesting in shaping the long-term behaviour of the system. Despite this, no existing work has considered the combined effects of the Cosner-type functional response and Michaelis-Menten-type harvesting. This represents a gap in understanding how hunting cooperation among predators and nonlinear harvesting affect population dynamics.

3. The Mathematical Model

A two-dimensional predator-prey model is constructed by defining $n(\tau)$ as the prey population and $p(\tau)$ as the predator population at time τ.

3.1. *Model Formulation*

The two-dimensional predator-prey model with a Cosner-type functional response was proposed by Ryu *et al.* (2018) and is given by

$$\begin{aligned} \frac{dn}{d\tau} &= rn\left(1-\frac{n}{k}\right) - \frac{Se_0np^2}{1+hSe_0np}, \\ \frac{dp}{d\tau} &= \frac{\varepsilon Se_0np^2}{1+hSe_0np} - \mu p. \end{aligned} \tag{3}$$

The model was derived from the classical Lotka-Volterra predator-prey model, where the prey growth rate, r, has a positive impact on the prey population, while the predator-prey interaction contributes positively to the predator population and negatively to the prey population. In addition, the natural mortality rate, μ, has a negative impact on the predator population. The model proposed by Ryu *et al.* (2018) can be extended by incorporating Michaelis-Menten-type nonlinear harvesting as follows:

$$\begin{aligned} \frac{dn}{d\tau} &= rn\left(1-\frac{n}{k}\right) - \frac{Se_0np^2}{1+hSe_0np} - \frac{qEn}{m_1E+m_2n}, \\ \frac{dp}{d\tau} &= \frac{\varepsilon Se_0np^2}{1+hSe_0np} - \mu p. \end{aligned} \tag{4}$$

All parameters in system (4) are assumed to be positive, and their descriptions are summarised in Table 1.

Table 1: Description of the parameters used in the model

Parameter	Description
r	Intrinsic growth rate of prey
k	Environmental carrying capacity for prey
S	Number of prey captured by a predator per encounter
e_0	Handling time required for each prey
h	Total encounter coefficient between prey and predator
q	Catchability coefficient
E	Harvesting effort
m_1	Limitation in harvesting effort
m_2	Limitation in stock size
ε	Energy conversion rate from prey to predator
μ	Natural mortality rate of the predator

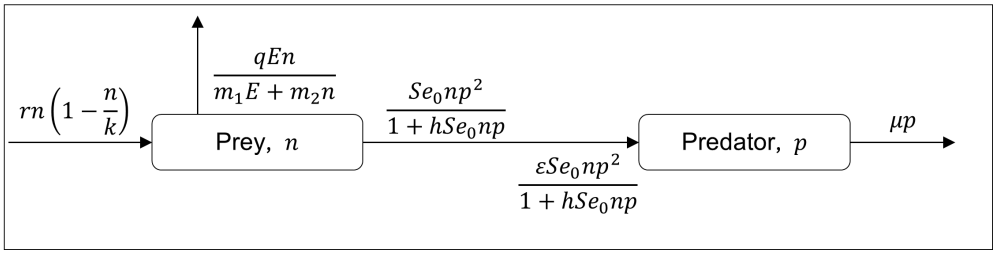

Figure 1: Schematic diagram showing the relationship between the prey and the predator

The term

$$rn\left(1-\frac{n}{k}\right)$$

represents the logistic growth rate of the prey population, bounded by the environmental carrying capacity, such as food availability. The term

$$\frac{Se_0np^2}{1+hSe_0np}$$

represents the interaction between the predator and prey populations through the Cosner-type functional response, which accounts for predator cooperation during hunting. The predator population is assumed to decline naturally at mortality rate μ when prey is absent.

Based on model (3), Shang *et al.* (2021b) and Mulugeta *et al.* (2024) extended the model by incorporating constant and proportional harvesting, respectively. Distinct from these models, the present study advances the model by introducing Michaelis-Menten-type nonlinear harvesting,

$$\frac{qEn}{m_1E+m_2n},$$

into the prey equation, thereby capturing more realistic and complex dynamics. The biological interactions incorporated in the model are illustrated in Figure 1. In Figure 1, arrows pointing towards a population indicate increases in its density, whereas arrows pointing away indicate decreases.

3.2. *Nondimensionalisation*

Following the formulation of the dimensional predator-prey model in system (4), nondimensionalisation is performed to reduce the number of parameters. By introducing the scaled variables

$$N=\frac{n}{A},\quad P=\frac{p}{B},\quad t=\frac{\tau}{C},$$

where A, B and C are positive scaling constants to be determined, the time derivatives become

$$\frac{dn}{d\tau}=\frac{A}{C}\frac{dN}{dt},\qquad \frac{dp}{d\tau}=\frac{B}{C}\frac{dP}{dt}.$$

Substituting these scaled variables into system (4) and choosing

$$A=k,\qquad B=\frac{1}{hkSe_0},\qquad C=\frac{1}{r},$$

the system is nondimensionalised as

$$\begin{aligned}\frac{dN}{dt}&=N(1-N)-\frac{aNP^2}{1+NP}-\frac{bN}{c+N},\\ \frac{dP}{dt}&=\frac{fNP^2}{1+NP}-gP.\end{aligned}\tag{5}$$

The dimensionless parameters are defined as

$$a = \frac{1}{rh^2k^2Se_0}, \qquad b = \frac{qE}{rm_2k}, \qquad c = \frac{m_1E}{m_2k}, \qquad f = \frac{\varepsilon}{rh}, \qquad g = \frac{\mu}{r}.$$

Here, a represents the dimensionless predation rate, b represents the dimensionless harvesting rate, c represents the dimensionless harvesting saturation rate, f represents the dimensionless energy conversion efficiency from prey to predator, and g represents the dimensionless predator mortality rate.

4. Equilibria and Stability Properties

This section focuses on determining the types of equilibrium points of system (5), followed by the local stability analysis of each equilibrium point.

4.1. *Equilibrium Points*

By considering the dynamics in the region

$$\mathbb{R}^2_+ = \{(N, P) : N \geq 0,\ P \geq 0\},$$

system (5) exhibits three types of equilibrium points:

(a) The extinction equilibrium point,

$$E_0 = (0, 0).$$

(b) The predator-free equilibrium points,

$$E_1^{\pm} = \left(\frac{1 - c \pm \sqrt{c^2 + 2c + 1 - 4b}}{2}, 0 \right),$$

which exist when

$$c^2 + 2c + 1 - 4b \geq 0$$

and the corresponding prey component is nonnegative.

(c) The coexistence equilibrium points,

$$E_2 = (\hat{N}, \hat{P}),$$

where

$$\hat{P} = \frac{g}{\hat{N}(f - g)}$$

and $\hat{N}$ is a positive solution of

$$\hat{N}^4 + \hat{N}^3(c - 1) + \hat{N}^2(b - c) + \frac{ag^2}{f(f - g)}\hat{N} + \frac{ag^2c}{f(f - g)} = 0. \tag{6}$$

The coexistence equilibrium exists when $f > g$ and the above equation has a positive solution $\hat{N} > 0$.

Equation (6) is obtained by setting system (5) equal to zero. From $\frac{dP}{dt} = 0$, it follows that

$$\hat{P} = \frac{g}{\hat{N}(f-g)}.$$

Substituting this expression into $\frac{dN}{dt} = 0$ yields equation (6).

4.2. *Local Stability Analysis*

Local stability is determined by analysing the Jacobian matrix of system (5) evaluated at each equilibrium point. This analysis is essential for bifurcation studies because it provides the conditions under which bifurcations may occur when system parameters are varied. Hence, understanding local stability is crucial for identifying thresholds at which the stability of equilibrium points changes. The Jacobian matrix at any arbitrary point (N, P) is given by

$$J(N,P) = \begin{bmatrix} 1 - 2N - \dfrac{aP^2}{(1+NP)^2} - \dfrac{bc}{(c+N)^2} & -\dfrac{2aNP + aN^2P^2}{(1+NP)^2} \\ \dfrac{fP^2}{(1+NP)^2} & \dfrac{2fNP + fN^2P^2}{(1+NP)^2} - g \end{bmatrix}. \tag{7}$$

4.2.1. *Extinction Equilibrium Point, E_0*

To analyse the local stability of the extinction equilibrium point E_0, the Jacobian matrix of the system at $E_0 = (0, 0)$ is evaluated as

$$J_0 = \begin{bmatrix} 1 - \dfrac{b}{c} & 0 \\ 0 & -g \end{bmatrix}. \tag{8}$$

From the Jacobian matrix in (8), the corresponding eigenvalues are

$$\lambda_1 = -g, \qquad \lambda_2 = \frac{c-b}{c}.$$

Since all parameters are positive, $\lambda_1 < 0$. Therefore, the extinction equilibrium point E_0 is locally asymptotically stable if $c < b$ and unstable if $c > b$.

4.2.2. *Predator-Free Equilibrium Points, $E_1^{\pm}$*

Theorem 4.1. *System* (5) *possesses predator-free equilibrium points*

$$E_1^{\pm} = \left(\frac{1 - c \pm \sqrt{c^2 + 2c + 1 - 4b}}{2}, 0 \right),$$

provided that these points exist in $\mathbb{R}^2_+$. Let

$$D = \sqrt{c^2 + 2c + 1 - 4b}.$$

Then $E_1^{\pm}$ is locally asymptotically stable if

$$c \mp D - \frac{4cb}{(c+1 \pm D)^2} < 0. \tag{9}$$

Otherwise, $E_1^{\pm}$ is unstable.

Proof. The Jacobian matrix evaluated at the predator-free equilibrium points $E_1^{\pm}$ is

$$J_1^{\pm} = \begin{bmatrix} c \mp D - \dfrac{4cb}{(c+1 \pm D)^2} & 0 \\ 0 & -g \end{bmatrix}, \tag{10}$$

where

$$D = \sqrt{c^2 + 2c + 1 - 4b}.$$

The eigenvalues of $J_1^{\pm}$ are

$$\lambda_1 = c \mp D - \frac{4cb}{(c+1 \pm D)^2}, \qquad \lambda_2 = -g.$$

Since $g > 0$, we have $\lambda_2 < 0$. Therefore, both eigenvalues have negative real parts if condition (9) holds. Hence, the predator-free equilibrium points $E_1^{\pm}$ are locally asymptotically stable if condition (9) is satisfied, and unstable otherwise.

4.2.3. *Coexistence Equilibrium Point, E_2*

Theorem 4.2. *Let $E_2 = (\hat{N}, \hat{P})$ be a coexistence equilibrium point of system* (5)*, where $\hat{N} > 0$ and $\hat{P} > 0$. Then E_2 is locally asymptotically stable if*

$$z_1 > 0 \quad \textit{and} \quad z_2 > 0,$$

where

$$\begin{aligned} z_1 =& \frac{1}{f^2(c+\hat{N})^2\hat{N}^2}\Big(-f^2gc^2\hat{N}^2 - 2f^2gc\hat{N}^3 - f^2g\hat{N}^4 + 2f^2c^2\hat{N}^3 \\ &+ 4f^2c\hat{N}^4 + 2f^2\hat{N}^5 + fg^2c^2\hat{N}^2 + 2fg^2c\hat{N}^3 + fg^2\hat{N}^4 + f^2bc\hat{N}^2 \\ &- f^2c^2\hat{N}^2 - 2f^2c\hat{N}^3 - f^2\hat{N}^4 + ag^2c^2 + 2ag^2c\hat{N} + ag^2\hat{N}^2\Big), \end{aligned} \tag{11}$$

and

$$\begin{aligned} z_2 =& \frac{g}{f^2(c+\hat{N})^2\hat{N}^2}\Big(-2f^2c^2\hat{N}^3 - 4f^2c\hat{N}^4 - 2f^2\hat{N}^5 + 2fgc^2\hat{N}^3 \\ &+ 4fgc\hat{N}^4 + 2fg\hat{N}^5 - f^2bc\hat{N}^2 + f^2c^2\hat{N}^2 + 2f^2c\hat{N}^3 + f^2\hat{N}^4 \\ &+ fgbc\hat{N}^2 - fgc^2\hat{N}^2 - 2fgc\hat{N}^3 - fg\hat{N}^4 + ag^2c^2 + 2ag^2c\hat{N} + ag^2\hat{N}^2\Big). \end{aligned} \tag{12}$$

Proof. The Jacobian matrix evaluated at the coexistence equilibrium point $E_2 = (\hat{N}, \hat{P})$ is

$$J_2 = \begin{bmatrix} j_1 & -\dfrac{ag(2f-g)}{f^2} \\ \dfrac{g^2}{f\hat{N}^2} & \dfrac{g(f-g)}{f} \end{bmatrix}, \tag{13}$$

where

$$\begin{aligned} j_1 = &- \frac{1}{\hat{N}^2 f^2 (c+\hat{N})^2} \Big(2f^2\hat{N}^5 + (4c-1)f^2\hat{N}^4 + 2f^2c(c-1)\hat{N}^3 \\ &+ \left(c(b-c)f^2 + ag^2 \right) \hat{N}^2 + 2ag^2c\hat{N} + ag^2c^2 \Big). \end{aligned}$$

The corresponding characteristic polynomial is

$$\lambda^2 + z_1\lambda + z_2 = 0, \tag{14}$$

where z_1 and z_2 are given in (11) and (12), respectively. By the Routh-Hurwitz criterion for a second-order polynomial, all eigenvalues of J_2 have negative real parts if and only if

$$z_1 > 0 \quad \text{and} \quad z_2 > 0.$$

Hence, the coexistence equilibrium point E_2 is locally asymptotically stable if conditions (11) and (12) hold. Otherwise, E_2 is not locally asymptotically stable.

5. Bifurcation Analysis

In this section, codimension-one bifurcations of system (5) with respect to the harvesting saturation rate c are examined analytically. Biologically, larger values of c indicate stronger saturation effects, making this parameter an important factor in the interaction between harvesting pressure and population dynamics. The analytical conditions for the occurrence of saddle-node and pitchfork bifurcations are obtained using Sotomayor's theorem (Perko 2001).

Theorem 5.1 (Sotomayor's theorem (Perko 2001))**.** *Consider the system*

$$\dot{\mathbf{x}} = \boldsymbol{\zeta}(\mathbf{x}, c),$$

where $\boldsymbol{\zeta}$ is a smooth function, $\mathbf{x} \in \mathbb{R}^n$ and c is the bifurcation parameter. Suppose that

$$\boldsymbol{\zeta}(\mathbf{x}_0, c_0) = \mathbf{0}$$

and the $n \times n$ Jacobian matrix

$$A = D\boldsymbol{\zeta}(\mathbf{x}_0, c_0)$$

has a simple eigenvalue $\lambda = 0$ with eigenvector v, whereas A^T has an eigenvector w corresponding to the eigenvalue $\lambda = 0$. Then the system exhibits the following bifurcations if the corresponding conditions are satisfied.

(1) Saddle-node bifurcation

(i) $w^T \boldsymbol{\zeta}_c(\mathbf{x}_0, c_0) \neq 0$,

(ii) $w^T \left[D^2\boldsymbol{\zeta}(\mathbf{x}_0, c_0)(v, v) \right] \neq 0$.

(2) Pitchfork bifurcation

(i) $w^T \boldsymbol{\zeta}_c(\mathbf{x}_0, c_0) = 0$,
(ii) $w^T \left[D\boldsymbol{\zeta}_c(\mathbf{x}_0, c_0)v\right] \neq 0$,
(iii) $w^T \left[D^2\boldsymbol{\zeta}(\mathbf{x}_0, c_0)(v, v)\right] = 0$,
(iv) $w^T \left[D^3\boldsymbol{\zeta}(\mathbf{x}_0, c_0)(v, v, v)\right] \neq 0$.

If the above conditions are satisfied, then the equilibrium point $\mathbf{x}_0$ *undergoes a saddle-node bifurcation or a pitchfork bifurcation at* $(\mathbf{x}_0, c_0)$*, respectively.*

Theorem 5.2 (Hopf bifurcation theorem (Perko 2001))**.** *Consider a smooth autonomous system of ordinary differential equations,*

$$\frac{d\mathbf{x}}{dt} = \boldsymbol{\zeta}(\mathbf{x}, c), \qquad \mathbf{x} \in \mathbb{R}^n, \quad c \in \mathbb{R}.$$

Suppose that for some parameter value c_0*, the system has an equilibrium point* $\mathbf{x}_0$*. Then a Hopf bifurcation occurs at* $(\mathbf{x}_0, c_0)$ *if the following conditions are satisfied:*

(1) Eigenvalue condition: The Jacobian matrix

$$J = D_{\mathbf{x}}\boldsymbol{\zeta}(\mathbf{x}_0, c_0)$$

has a pair of simple purely imaginary eigenvalues $\pm i\omega_0$*, where* $\omega_0 > 0$*, and all other eigenvalues have nonzero real parts.*

(2) Transversality condition: The real part of the eigenvalues, denoted by $\alpha(c)$*, crosses the imaginary axis, that is,*

$$\left.\frac{d\alpha(c)}{dc}\right|_{c=c_0} \neq 0.$$

If both conditions are satisfied, then the equilibrium point $\mathbf{x}_0$ *undergoes a Hopf bifurcation at* $(\mathbf{x}_0, c_0)$*, leading to oscillatory behaviour in the form of periodic solutions.*

5.1. *Pitchfork Bifurcation*

Theorem 5.3. *System* (5) *undergoes a pitchfork bifurcation at the extinction equilibrium point* $E_0 = (0, 0)$ *when*

$$c = c_{PF} = b = 1.$$

Proof. When $c = c_{PF} = b$, the Jacobian matrix evaluated at E_0 is

$$J(E_0; c_{PF}) = \begin{bmatrix} 0 & 0 \\ 0 & -g \end{bmatrix},$$

which has a simple zero eigenvalue. The eigenvectors corresponding to the zero eigenvalues of $J(E_0; c_{PF})$ and $J^T(E_0; c_{PF})$ are denoted by v and w, respectively, where

$$v = w = \begin{bmatrix} 1 \\ 0 \end{bmatrix}.$$

Let

$$\boldsymbol{\zeta}(N,P,c)=\begin{pmatrix} N(1-N)-\dfrac{aNP^2}{1+NP}-\dfrac{bN}{c+N} \\ \dfrac{fNP^2}{1+NP}-gP \end{pmatrix}.$$

Then

$$\begin{aligned}
\boldsymbol{\zeta}_c(E_0,c_{PF}) &= \begin{pmatrix}0\\0\end{pmatrix}, \\
D\boldsymbol{\zeta}_c(E_0,c_{PF})v &= \begin{pmatrix}1\\ \dfrac{1}{b}\\0\end{pmatrix}, \\
D^2\boldsymbol{\zeta}(E_0,c_{PF})(v,v) &= \begin{pmatrix}-2+\dfrac{2}{b}\\0\end{pmatrix}, \\
D^3\boldsymbol{\zeta}(E_0,c_{PF})(v,v,v) &= \begin{pmatrix}-\dfrac{6}{b^2}\\0\end{pmatrix}.
\end{aligned}$$

When $c=c_{PF}=b=1$, we obtain

$$\begin{aligned}
w^T\boldsymbol{\zeta}_c(E_0,c_{PF}) &= 0, \\
w^T\left[D\boldsymbol{\zeta}_c(E_0,c_{PF})v\right] &= 1\neq 0, \\
w^T\left[D^2\boldsymbol{\zeta}(E_0,c_{PF})(v,v)\right] &= 0, \\
w^T\left[D^3\boldsymbol{\zeta}(E_0,c_{PF})(v,v,v)\right] &= -6\neq 0.
\end{aligned}$$

Therefore, by Sotomayor's theorem (Perko 2001), system (5) undergoes a pitchfork bifurcation at $c=c_{PF}=b=1$.

5.2. *Saddle-Node Bifurcation*

Theorem 5.4. *System* (5) *undergoes a saddle-node bifurcation at the coexistence equilibrium point*

$$E_2=(\hat{N},\hat{P}),\qquad \hat{P}=\frac{g}{\hat{N}(f-g)},$$

when $c=c_{SN}$*, where*

$$\begin{aligned}
c_{SN}=&\frac{\hat{N}}{f^2(-4\hat{N}^3+2\hat{N}^2)+4\hat{N}^3fg-2\hat{N}^2fg+2ag^2}\Bigg(f^2\hat{N}\left(4\hat{N}^2+b-2\hat{N}\right)\\
&-fg\hat{N}\left(4\hat{N}^2+b-2\hat{N}\right)-2ag^2\\
&+\sqrt{-4bf\hat{N}(f-g)\left(-\frac{f^2\hat{N}\left(8\hat{N}^2+b-4\hat{N}\right)}{4}+\frac{fg\hat{N}\left(8\hat{N}^2+b-4\hat{N}\right)}{4}+ag^2\right)}\Bigg).
\end{aligned}$$

Proof. When $c = c_{SN}$, the determinant of the Jacobian matrix at E_2 satisfies

$$\det(J_{E_2}) = 0.$$

Hence, the Jacobian matrix has a simple zero eigenvalue. The eigenvectors corresponding to the zero eigenvalues of J_{E_2} and $J_{E_2}^T$ are denoted by v and w, respectively, where

$$v = \begin{bmatrix} \frac{\hat{N}^2(g-f)}{g} \\ 1 \end{bmatrix}, \qquad w = \begin{bmatrix} \frac{f(f-g)}{a(2f-g)} \\ 1 \end{bmatrix}.$$

Then

$$\boldsymbol{\zeta}_c(E_2, c_{SN}) = \begin{pmatrix} d_1 \\ 0 \end{pmatrix}, \qquad D^2\boldsymbol{\zeta}(E_2, c_{SN})(v, v) = \begin{pmatrix} d_2 \\ d_3 \end{pmatrix},$$

where

$$d_1 = \frac{4b\left(-2f(f-g)\hat{N}^3 + f(f-g)\hat{N}^2 + ag^2\right)^2}{\hat{N}\left(bf\hat{N}(f-g) + M\right)^2},$$

$$d_2 = \frac{\hat{N}^4(g-f)^2}{g^2}\left(-2 + \frac{2ag^3}{\hat{N}^3(f-g)^3\left(\frac{g}{f-g}+1\right)^3} - \frac{2bQ}{(\hat{N}+Q)^3}\right),$$

$$d_3 = -\frac{2(f-g)^2\left(f\hat{N}^2 - 2g\hat{N}^2 + g\right)}{f^2\hat{N}},$$

$$M = \sqrt{-4bf\hat{N}(f-g)\left(-\frac{f^2\hat{N}\left(8\hat{N}^2 + b - 4\hat{N}\right)}{4} + \frac{fg\hat{N}\left(8\hat{N}^2 + b - 4\hat{N}\right)}{4} + ag^2\right)},$$

$$Q = \frac{\hat{N}\left(f^2\hat{N}(4\hat{N}^2 + b - 2\hat{N}) - fg\hat{N}(4\hat{N}^2 + b - 2\hat{N}) - 2ag^2 + M\right)}{f^2(-4\hat{N}^3 + 2\hat{N}^2) + 4\hat{N}^3fg - 2\hat{N}^2fg + 2ag^2} = c_{SN}.$$

Thus,

$$w^T\boldsymbol{\zeta}_c(E_2, c_{SN}) = \frac{d_1 f(f-g)}{a(2f-g)} \neq 0,$$

$$w^T\left[D^2\boldsymbol{\zeta}(E_2, c_{SN})(v, v)\right] = \frac{d_2 f(f-g)}{a(2f-g)} + d_3 \neq 0.$$

Therefore, by Sotomayor's theorem (Perko 2001), system (5) undergoes a saddle-node bifurcation at $c = c_{SN}$, provided that $f \neq g$ and $2f \neq g$.

5.3. *Hopf Bifurcation*

The subsequent analysis focuses on verifying the occurrence of Hopf bifurcation at the coexistence equilibrium point E_2 using the Hopf bifurcation theorem.

Theorem 5.5. *System* (5) *undergoes a Hopf bifurcation at the coexistence equilibrium point*

$$E_2 = (\hat{N}, \hat{P})$$

when $c = c_{HB}$*, provided that*

$$\begin{aligned}\frac{1}{\left[\hat{N}f(c+\hat{N})\right]^2}\Big[&ag^2c^2 + 2ag^2c\hat{N} + 2f^2c\hat{N}^3(c-1) + 2f^2\hat{N}^5 \\ &+ f^2\hat{N}^4(4c-1) + \hat{N}^2\left(ag^2 + f^2c(b-c)\right)\Big] = \frac{g(f-g)}{f},\end{aligned} \tag{15}$$

$$\begin{aligned}\frac{g}{\left[\hat{N}f(c+\hat{N})\right]^2}\Big[&ag^2c^2 + 2ag^2c\hat{N} + ag^2\hat{N}^2 - f^2bc\hat{N}^2 - 2f^2c^2\hat{N}^3 \\ &+ f^2c^2\hat{N}^2 - 4f^2c\hat{N}^4 + 2f^2c\hat{N}^3 - 2f^2\hat{N}^5 + f^2\hat{N}^4 + fgbc\hat{N}^2 \\ &+ 2fgc^2\hat{N}^3 - fgc^2\hat{N}^2 + 4fgc\hat{N}^4 - 2fgc\hat{N}^3 + 2fg\hat{N}^5 - fg\hat{N}^4\Big] > 0,\end{aligned} \tag{16}$$

and the transversality condition

$$\frac{d}{dc}\operatorname{Tr}\left(J_{E_2(c)}\right)\Big|_{c=c_{HB}} \neq 0 \tag{17}$$

is satisfied.

Proof. The characteristic equation of system (5) at the coexistence equilibrium point E_2 is given by

$$\lambda^2 - \operatorname{Tr}(J_{E_2})\lambda + \det(J_{E_2}) = 0, \tag{18}$$

where

$$\begin{aligned}\operatorname{Tr}(J_{E_2}) =&\frac{g(f-g)}{f} - \frac{1}{\left[\hat{N}f(c+\hat{N})\right]^2}\Big[ag^2c^2 + 2ag^2c\hat{N} \\ &+ 2f^2c\hat{N}^3(c-1) + 2f^2\hat{N}^5 + f^2\hat{N}^4(4c-1) + \hat{N}^2\left(ag^2 + f^2c(b-c)\right)\Big],\end{aligned}$$

and

$$\begin{aligned}\det(J_{E_2}) =&\frac{g}{\left[\hat{N}f(c+\hat{N})\right]^2}\Big[ag^2c^2 + 2ag^2c\hat{N} + ag^2\hat{N}^2 - f^2bc\hat{N}^2 \\ &- 2f^2c^2\hat{N}^3 + f^2c^2\hat{N}^2 - 4f^2c\hat{N}^4 + 2f^2c\hat{N}^3 - 2f^2\hat{N}^5 \\ &+ f^2\hat{N}^4 + fgbc\hat{N}^2 + 2fgc^2\hat{N}^3 - fgc^2\hat{N}^2 + 4fgc\hat{N}^4 \\ &- 2fgc\hat{N}^3 + 2fg\hat{N}^5 - fg\hat{N}^4\Big].\end{aligned}$$

Condition (15) is equivalent to

$$\mathrm{Tr}(J_{E_2}) = 0.$$

Together with condition (16), we have

$$\mathrm{Tr}(J_{E_2}) = 0 \quad \text{and} \quad \det(J_{E_2}) > 0.$$

Hence, the characteristic equation (18) has a pair of purely imaginary eigenvalues

$$\lambda_{1,2} = \pm i\sqrt{\det(J_{E_2)}},$$

which satisfies the eigenvalue condition of the Hopf bifurcation theorem.

It remains to verify the transversality condition. For a two-dimensional system, the real part of the conjugate eigenvalues is given by

$$\alpha(c) = \frac{1}{2}\,\mathrm{Tr}\left(J_{E_2(c)}\right).$$

Thus,

$$\left.\frac{d\alpha(c)}{dc}\right|_{c=c_{HB}} = \frac{1}{2}\,\frac{d}{dc}\,\mathrm{Tr}\left(J_{E_2(c)}\right)\Big|_{c=c_{HB}}.$$

Therefore, if condition (17) holds, then

$$\left.\frac{d\alpha(c)}{dc}\right|_{c=c_{HB}} \neq 0.$$

By the Hopf bifurcation theorem 5.2, system (5) undergoes a Hopf bifurcation at the coexistence equilibrium point E_2 when $c = c_{HB}$.

6. Numerical Simulations

Numerical simulations are conducted to examine the dynamical behaviours of system (5) using both MATLAB and MatCont software. In these simulations, the harvesting saturation rate c is used as the bifurcation parameter to explore its effect on system dynamics. Time series simulations are carried out using two sets of initial conditions, namely $(N(0), P(0)) = (0.1, 0.5)$ and $(N(0), P(0)) = (0.4, 2.5)$. All parameter values are chosen for the purpose of numerical investigation and are summarised in Table 2. The study is limited to the parameter setting given in this table throughout the analysis.

Table 2: Parameter values of system (5)

Parameter	**Value**
a	0.1000
b	1.0000
c	3.0000 (varied)
f	0.2000
g	0.1000

Figures 2(a) and 2(b) show the codimension-one bifurcation diagrams of system (5) with

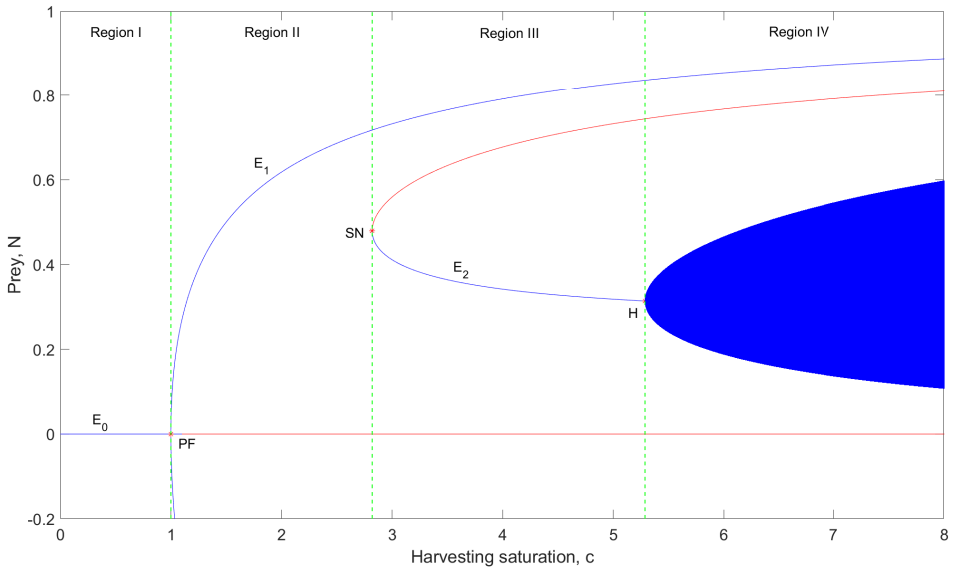

(a) N against c

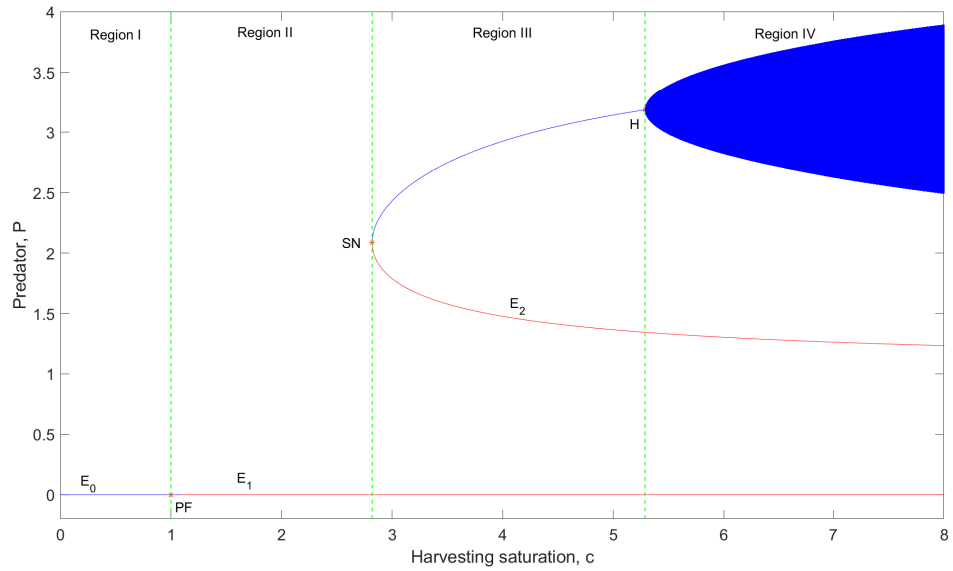

(b) P against c

Figure 2: Codimension-one bifurcation diagram of system (5) with respect to the harvesting saturation rate c for (a) prey population N and (b) predator population P

respect to the harvesting saturation rate c for the prey population N and predator population P, respectively. The blue solid line denotes a stable equilibrium, while the red solid line indicates an unstable equilibrium. The green dotted lines divide the bifurcation diagrams into four distinct regions, each representing a different level of harvesting saturation, as follows:

(1) Region I: $0.0000 \leq c < 1.0000$,
(2) Region II: $1.0000 \leq c < 2.8205$,
(3) Region III: $2.8205 \leq c < 5.2883$,
(4) Region IV: $5.2883 \leq c < 8.0000$.

The harvesting saturation rate increases progressively from Region I, which reflects an extremely low saturation rate, to Region IV, which corresponds to an extremely high saturation rate. Referring to Figure 2, system (5) exhibits three types of bifurcations, namely supercritical pitchfork bifurcation, denoted by PF, saddle-node bifurcation, denoted by SN, and supercritical Hopf bifurcation, denoted by H. The supercritical pitchfork bifurcation occurs at $c = 1.0000$, where a stable equilibrium point loses its stability and branches into two equilibria. The saddle-node bifurcation takes place at $c = 2.8205$, where a pair of equilibria with opposite stability is created as the harvesting saturation rate c passes through this critical value. Meanwhile, the supercritical Hopf bifurcation occurs at $c = 5.2883$, where a stable equilibrium loses its stability and gives rise to stable limit cycles.

In Figure 2, Region I corresponds to an extremely low harvesting saturation rate. In this region, there is only one stable extinction equilibrium point, E_0, in the positive region, as shown in Figure 3. This result is consistent with the analytical condition indicating that E_0 is locally asymptotically stable when $c < b$. This indicates that under very low saturation rates, both prey and predator populations are more likely to go extinct, as shown in Figure 4. Mathematically, a low value of the harvesting saturation rate c reflects a high level of harvesting. This implies that the harvesting rate does not saturate easily, allowing prey to be removed effectively regardless of their abundance. As a result, the prey population is harvested rapidly, leaving insufficient food to sustain the predator population. This imbalance eventually leads to the extinction of both species.

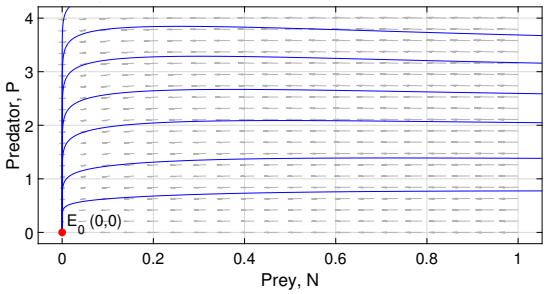

Figure 3: Phase portrait at $c = 0.5$ in Region I

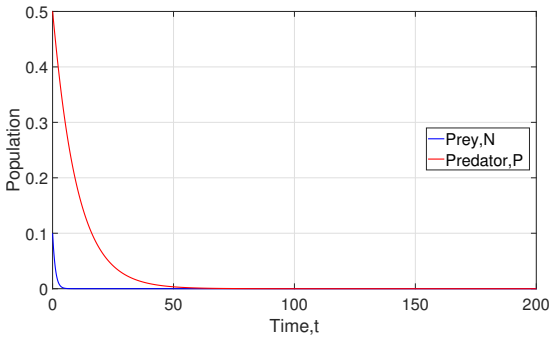

Figure 4: Time series at $c = 0.5$ with $(N(0), P(0)) = (0.1, 0.5)$ in Region I

As the harvesting saturation rate increases from Region I to Region II, the stable extinction equilibrium point E_0 undergoes a supercritical pitchfork bifurcation at the critical value $c = 1.0000$, in agreement with Theorem 5.3. Once the parameter value crosses this threshold, E_0 loses its stability and branches into two predator-free equilibria, $E_1^{\pm}$. However, one of these equilibria lies in the negative region and is therefore biologically not meaningful. Consequently, in Region II, only one biologically feasible stable predator-free equilibrium remains, as shown

in Figure 5. Furthermore, the extinction equilibrium point E_0 remains unstable, while the biologically feasible predator-free equilibrium point remains stable for $c > 1.0000$, consistent with the analytical stability conditions derived in Section 4.2 and Theorem 4.1. In other words, the prey population can persist in the long run, whereas the predator population becomes extinct, as shown in Figure 6.

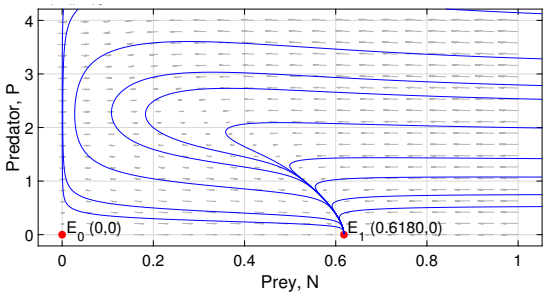

Figure 5: Phase portrait at $c = 2$ in Region II

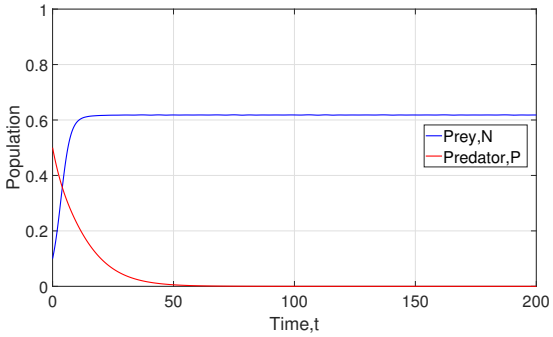

Figure 6: Time series at $c = 2$ with $(N(0), P(0)) = (0.1, 0.5)$ in Region II

Moving from Region II to Region III, which indicates a high harvesting saturation rate, the coexistence equilibrium point

$$E_2 = (0.4793, 2.0864)$$

undergoes a saddle-node bifurcation at $c = 2.8205$, in agreement with Theorem 5.4. This bifurcation leads to the formation of a pair of equilibria with opposite stability. Interestingly, due to the emergence of the stable coexistence equilibrium point E_2, two stable equilibria, namely E_1 and E_2, are observed in Region III, as shown in Figure 7. This phenomenon is referred to as bistability. As a result, the solution of the system may converge to either equilibrium depending on the initial condition, as shown in Figures 8a and 8b.

Notably, the coexistence equilibrium point E_2 exists and is stable for $2.8205 < c < 5.2883$, in agreement with Theorem 4.2. For example, at $c = 4$, the stability conditions are satisfied with $z_1 = 0.1782 > 0$ and $z_2 = 0.0108 > 0$. Hence, the eigenvalues

$$\lambda_1 = -0.0891 + 0.0531i \quad \text{and} \quad \lambda_2 = -0.0891 - 0.0531i$$

have negative real parts, indicating that E_2 is locally asymptotically stable. Therefore, to ensure the coexistence of both species, the harvesting saturation rate must remain within this range to prevent species extinction.

From Figure 2, Region IV shows that the stable coexistence equilibrium point E_2 undergoes a supercritical Hopf bifurcation and gives rise to a stable limit cycle at $c = 5.2883$, in agreement

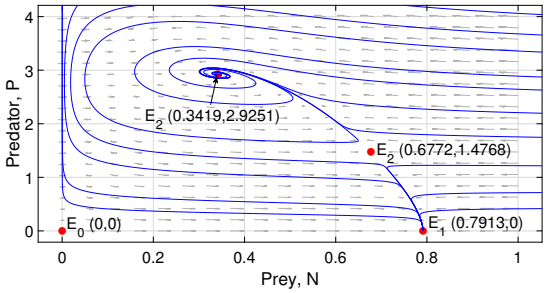

Figure 7: Phase portrait at $c = 4$ in Region III

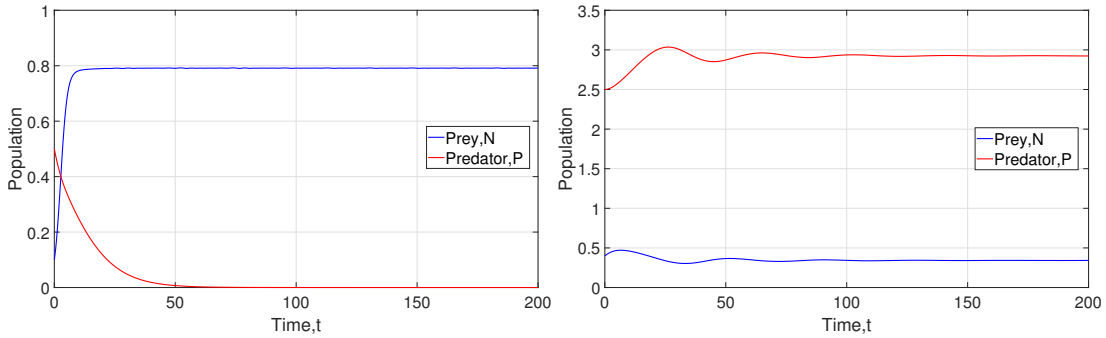

(a) $(N(0), P(0)) = (0.1, 0.5)$ (b) $(N(0), P(0)) = (0.4, 2.5)$

Figure 8: Time series at $c = 4$ in Region III

with Theorem 5.5. In this region, the unstable coexistence equilibrium point E_2 is surrounded by stable limit cycles, and the amplitude of these stable limit cycles continues to increase as the parameter c increases. The appearance of the limit cycle results in oscillatory behaviour in both predator and prey populations, as shown in Figure 10b. Similar to Region III, Region IV also exhibits bistability due to the presence of a stable limit cycle and a stable predator-free equilibrium point E_1, as shown in Figure 9. Therefore, the survival of both species strongly depends on the initial conditions, as illustrated in Figures 10a and 10b.

Numerical simulations indicate that the limit cycles persist beyond $c > 300$. However, such extreme values of c are biologically unrealistic, as they imply persistently weak harvesting saturation far beyond realistic ecological conditions. Therefore, the analysis is restricted to $c \leq 8$, which preserves ecological relevance while capturing the key dynamical aspects.

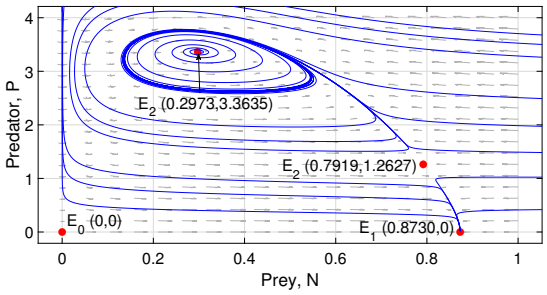

Figure 9: Phase portrait at $c = 7$ in Region IV

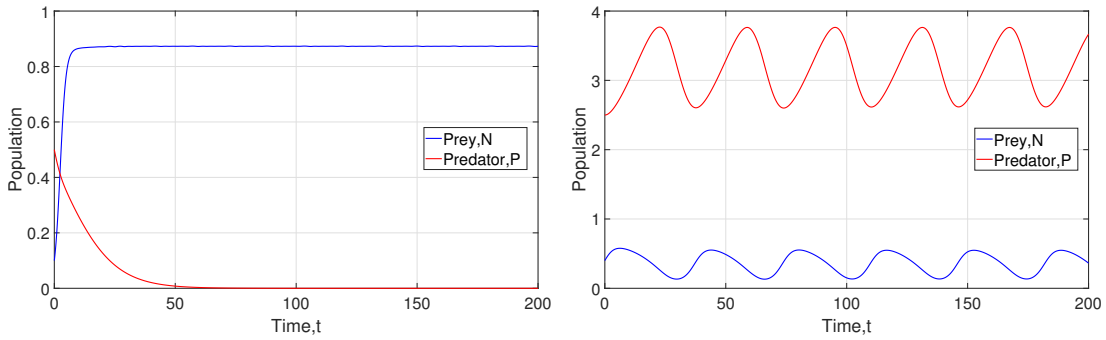

(a) $(N(0), P(0)) = (0.1, 0.5)$ (b) $(N(0), P(0)) = (0.4, 2.5)$

Figure 10: Time series at $c = 7$ in Region IV

7. Results and Discussion

System (5) exhibits complex dynamical behaviours driven by the interaction between the Cosner-type functional response and Michaelis-Menten-type prey harvesting. The Cosner-type functional response models cooperative hunting among predators, while Michaelis-Menten-type harvesting captures saturation effects due to practical limitations. These two realistic mechanisms give rise to complex transitions as the harvesting saturation rate c increases.

At low values of c, the system possesses only the extinction equilibrium point E_0. This indicates that highly efficient harvesting leads to population extinction. A supercritical pitchfork bifurcation then destabilises E_0 and gives rise to a stable predator-free equilibrium point E_1, where the prey population survives while the predator population becomes extinct. This marks the critical point at which the prey population can persist under reduced harvesting pressure. Further increasing c triggers a saddle-node bifurcation, giving rise to two coexistence equilibria with opposite stability. The coexistence of the stable predator-free equilibrium point E_1 and the stable coexistence equilibrium point E_2 introduces bistability, where the long-term survival of the species depends on the initial conditions. At extremely high values of c, a supercritical Hopf bifurcation occurs, causing E_2 to become unstable and giving rise to a stable limit cycle. This leads to another bistable region involving the stable predator-free equilibrium point E_1 and a stable limit cycle.

These bifurcations with respect to the harvesting saturation rate c lead to multiple bistable regions in the system. For moderate values of c, bistability arises between the stable coexistence equilibrium and the stable predator-free equilibrium. At higher values of c, bistability occurs between the stable predator-free equilibrium and stable limit cycles. In both cases, species survival is highly dependent on the initial population densities. This behaviour is consistent with observed ecological thresholds, where minor changes in population density or harvesting effort can trigger abrupt shifts in population dynamics. Bistability phenomena have been observed in many experimental studies. For example, Scheffer *et al.* (2001) showed that shallow lakes can abruptly shift between clear and turbid states depending on nutrient input, illustrating bistability. In fisheries, Mullon *et al.* (2005) reported that overexploited fish stocks may collapse below a critical threshold but can recover if conditions improve. These real-world scenarios support the biological relevance of the bistable regions observed in the present model.

Compared to other predator-prey models, the present system captures richer dynamical outcomes. Ryu *et al.* (2018) considered a predator-prey model incorporating a Cosner-type functional response, and their system exhibits saddle-node and Hopf bifurcations under varying predation rates. Similar results were obtained by Gupta and Chandra (2013), who analysed a modified Leslie-Gower predator-prey model with Michaelis-Menten-type prey harvesting. Their model was shown to exhibit saddle-node, transcritical and Hopf bifurcations of codi-

mension one. In terms of codimension-one bifurcations, the present model produces richer dynamics, including saddle-node, Hopf and pitchfork bifurcations, when Michaelis-Menten-type prey harvesting is incorporated with the Cosner-type functional response. The pitchfork bifurcation observed in this system is particularly important because it involves the emergence of multiple equilibrium branches. From an application standpoint, pitchfork bifurcations are informative because they capture scenarios in which a population system may split into multiple possible long-term outcomes. This makes the bifurcation structure of the present model richer and more interesting.

8. Conclusion

This paper investigated a two-dimensional predator-prey model with Michaelis-Menten-type prey harvesting and a Cosner-type functional response. The Cosner-type functional response is particularly worth studying because it provides a biologically grounded mechanism for capturing the nonlinear effects of predator cooperation during predation. The model exhibits three types of equilibrium points, namely extinction, predator-free and coexistence equilibria. Furthermore, the stability of each equilibrium point was analysed. Through analytical and numerical investigations, the model was shown to exhibit three types of codimension-one bifurcations, namely supercritical pitchfork, saddle-node and supercritical Hopf bifurcations. These bifurcations mark the stability transitions between extinction, predator-free and coexistence equilibria as the harvesting saturation rate c varies.

At a very low harvesting saturation rate, the system admits only one stable extinction equilibrium point, E_0, suggesting that highly efficient harvesting drives both species to extinction. As the harvesting saturation rate increases, a supercritical pitchfork bifurcation leads to the emergence of a stable predator-free equilibrium point, E_1, where the prey population persists but the predator population becomes extinct. A further increase in the harvesting saturation rate triggers a saddle-node bifurcation that introduces a stable coexistence equilibrium point, E_2, resulting in bistability between the predator-free and coexistence states. Hence, the long-term population outcomes depend strongly on the initial conditions. At high harvesting saturation levels, the coexistence equilibrium point undergoes a supercritical Hopf bifurcation and gives rise to stable limit cycles. The emergence of stable limit cycles and a stable predator-free equilibrium point gives rise to another bistability phenomenon.

In summary, at low harvesting saturation rates, both populations face extinction, while at higher saturation levels, the prey population can survive, but predator persistence depends on the initial population sizes, leading to multiple possible long-term outcomes. Overall, the results demonstrate how nonlinear harvesting and the Cosner-type functional response interact to produce complex dynamics, including bistability and population oscillations. These findings highlight the importance of harvesting saturation thresholds in determining long-term species persistence.

Acknowledgement

The first author gratefully acknowledges financial support from the MyBrain 2.0 scholarship programme, sponsored by the Ministry of Higher Education Malaysia.

References

Alves M.T. & Hilker F.M. 2017. Hunting cooperation and Allee effects in predators. *Journal of Theoretical Biology* **419**: 13–22.

Berec L. 2010. Impacts of foraging facilitation among predators on predator-prey dynamics. *Bulletin of Mathematical Biology* **72**(1): 94–121.

Clark C.W. & Mangel M. 1979. Aggregation and fishery dynamics: A theoretical study of schooling and the purse seine tuna fisheries. *Fishery Bulletin* **77**(2): 317–337.

Cosner C., DeAngelis D.L., Ault J.S. & Olson D.B. 1999. Effects of spatial grouping on the functional response of predators. *Theoretical Population Biology* **56**: 65–75.

Debnath S., Majumdar P., Sarkar S. & Ghosh U. 2022. Global dynamics of a prey–predator model with Holling type III functional response in the presence of harvesting. *Journal of Biological Systems* **30**(01): 225–260.

Eshkuvatov Z., Laadjal Z. & Ismail S. 2021. Numerical treatment of nonlinear mixed Volterra-Fredholm integro-differential equations of fractional order. *AIP Conference Proceedings*, p. 020006.

Eshkuvatov Z., Laadjal Z. & Ismail S. 2025. Solving class of mixed nonlinear multi-term fractional Volterra-Fredholm integro-differential equations by new development of HAM. *Mathematical Modelling and Analysis* **30**(1): 52–73.

Gupta R. & Chandra P. 2013. Bifurcation analysis of modified Leslie–Gower predator–prey model with Michaelis–Menten type prey harvesting. *Journal of Mathematical Analysis and Applications* **398**(1): 278–295.

Holling C.S. 1959. Some characteristics of simple types of predation and parasitism. *The Canadian Entomologist* **91**(7): 385–398.

Kashyap A.J., Zhu Q., Sarmah H.K. & Bhattacharjee D. 2023. Dynamical study of a predator-prey system with Michaelis-Menten type predator-harvesting. *International Journal of Biomathematics* **16**(08): 2250135.

Kumbhakar R., Pal S., Pal N. & Tiwari P.K. 2023. Bistability and tristability in a predator-prey model with strong Allee effect in prey. *Journal of Biological Systems* **31**(01): 215–243.

MacNulty D.R., Tallian A., Stahler D.R. & Smith D.W. 2014. Influence of group size on the success of wolves hunting bison. *PLOS ONE* **9**(11): e112884.

Majumdar P., Debnath S., Sarkar S. & Ghosh U. 2021. The complex dynamical behavior of a prey-predator model with Holling type-III functional response and non-linear predator harvesting. *International Journal of Modelling and Simulation* **42**(2): 287–304.

Mech L.D. 1970. *The Wolf: The Ecology and Behavior of an Endangered Species*. Garden City, New York: The Natural History Press.

Mortuja M., Chaube M. & Kumar S. 2025. Dynamic analysis of a predator-prey model with Michaelis-Menten prey harvesting and hunting cooperation in predators. *Journal of Applied Mathematics and Computing* **71**: 6207–6229.

Moussaoui A. & Auger P. 2021. A bioeconomic model of a fishery with saturated catch and variable price: Stabilizing effect of marine reserves on fishery dynamics. *Ecological Complexity* **45**: 100906.

Mullon C., Fréon P. & Cury P. 2005. The dynamics of collapse in world fisheries. *Fish and Fisheries* **6**(2): 111–120.

Mulugeta B.T., Ren J., Yuan Q. & Yu L. 2024. Bifurcation analysis of predator–prey model with Cosner type functional response and combined harvesting. *Mathematical Methods in the Applied Sciences* **47**(6): 5286–5306.

Perko L. 2001. *Differential Equations and Dynamical Systems*. 3rd Ed. New York: Springer-Verlag.

Roy S. & Tiwari P.K. 2025. Bistability in a predator-prey model characterized by the Crowley-Martin functional response: Effects of fear, hunting cooperation, additional foods and nonlinear harvesting. *Mathematics and Computers in Simulation* **228**: 274–297.

Ryu K., Ko W. & Haque M. 2018. Bifurcation analysis in a predator–prey system with a functional response increasing in both predator and prey densities. *Nonlinear Dynamics* **94**: 1639–1656.

Scheffer M., Carpenter S., Foley J.A., Folke C. & Walker B. 2001. Catastrophic shifts in ecosystems. *Nature* **413**(6856): 591–596.

Shang Z., Qiao Y., Duan L. & Miao J. 2021a. Bifurcation analysis and global dynamics in a predator–prey system of Leslie type with an increasing functional response. *Ecological Modelling* **455**: 109660.

Shang Z., Qiao Y., Duan L. & Miao J. 2021b. Bifurcation analysis in a predator–prey system with an increasing functional response and constant-yield prey harvesting. *Mathematics and Computers in Simulation* **190**: 976–1002.

Shao Y. & Kong W. 2022. A predator-prey model with Beddington-DeAngelis functional response and multiple delays in deterministic and stochastic environments. *Mathematics* **10**(18): 3378.

Xie B., Zhang Z. & Zhang N. 2021. Influence of the fear effect on a Holling type II prey-predator system with a Michaelis-Menten type harvesting. *International Journal of Bifurcation and Chaos* **31**(14): 2150216.

Yang R., Song Q. & An Y. 2022. Spatiotemporal dynamics in a predator-prey model with functional response increasing in both predator and prey densities. *Mathematics* **10**(1): 17.

Department of Mathematical Sciences
Faculty of Science
Universiti Teknologi Malaysia
81310 UTM Skudai
Johor, MALAYSIA
E-mail: huiyichen001123@gmail.com, taukeong@utm.my[*]

Received: 8 July 2025
Accepted: 30 January 2026

[*]Corresponding author